

Theory of topological quantum phase transitions in 3D noncentrosymmetric systems

Bohm-Jung Yang,¹ Mohammad Saeed Bahramy,¹ Ryotaro Arita,^{1,2} Hiroki Isobe,² Eun-Gook Moon,³ and Naoto Nagaosa^{1,2}

¹RIKEN Center for Emergent Matter Science, Wako, Saitama 351-0198, Japan

²Department of Applied Physics, University of Tokyo, Tokyo 113-8656, Japan

³Department of Physics, University of California, Santa Barbara, CA 93106, USA

(Dated: September 14, 2018)

We have constructed a general theory describing the topological quantum phase transitions in 3D systems with broken inversion symmetry. While the consideration of the system's codimension generally predicts the appearance of a stable metallic phase between the normal and topological insulators, it is shown that a direct topological phase transition between two insulators is also possible when an accidental band crossing (ABC) occurs along directions with high crystalline symmetry. At the quantum critical point (QCP), the energy dispersion becomes quadratic along one direction while the dispersions along the other two orthogonal directions are linear, which manifests the zero chirality of the band touching point (BTP). Due to the anisotropic dispersion at QCP, various thermodynamic and transport properties show unusual temperature dependence and anisotropic behaviors.

PACS numbers:

The 3D topological insulator (TI) is a new state of matter in which the nontrivial topology of bulk electronic wave functions guarantees the existence of gapless states on the sample's boundary. [1, 2] Because of its topological nature, the surface gapless states are protected against small perturbations preserving the time-reversal symmetry (TRS) as long as the bulk band gap remains finite. Therefore to change the bulk topological property, the band gap should be closed at some points in the Brillouin zone (BZ) via accidental band crossing (ABC). Recently, such a topological phase transition (PT) is realized in $\text{BiTl}(\text{S}_{1-x}\text{Se}_x)_2$ [3, 4], by modulating the spin-orbit interaction or the crystal lattice. In inversion symmetric systems such as $\text{BiTl}(\text{S}_{1-x}\text{Se}_x)_2$, the topological PT can be described by the (3+1) dimensional massive Dirac Hamiltonian in general. In this sense, the topological PT of 3D TIs provides a new venue to study intriguing quantum critical behaviors of 3D particles with relativistic dispersion. [5, 6, 23]

On the other hand, for noncentrosymmetric systems, our understanding of the topological PT and corresponding quantum critical behavior is still incomplete. By considering the codimension for ABC, a stable metallic phase was predicted to appear between TI and normal insulator in 3D noncentrosymmetric systems. [8] The intervening metallic phase, dubbed a Weyl semi-metal, has topological stability because there are several gapless points (Weyl points) with nonzero chiral charge at the Fermi level. [9] Therefore before every Weyl point is annihilated by colliding with another Weyl point with opposite chiral charge, the Weyl semi-metal should stably survive across the PT. In this respect, the recent discovery of a direct PT between two insulators in noncentrosymmetric compound BiTeI is an unexpected surprise. [10–12] At the QCP of BiTeI , instead of a Weyl semi-metal, several isolated band touching points (BTPs) with anisotropic dispersion appear, which suggests the diversity of the possible phase diagrams of noncentrosymmetric systems accessible via ABC.

In this paper, we propose generic phase diagrams for 3D noncentrosymmetric systems that can be achieved through

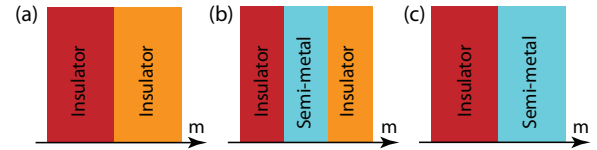


FIG. 1: (Color online) Generic phase diagrams, resulting from ABC between conduction and valence bands in 3D noncentrosymmetric systems. Here m indicates an external control parameter.

ABC, as depicted in Fig. 1. We carry out the analysis of the minimal two-band Hamiltonian describing the ABC to derive the conditions for these insulator-to-metal and insulator-to-insulator transitions (IIT). The key ingredient to obtain Fig. 1 is the fact that the chirality of the BTP at QCP is zero. Therefore it can be either gapped out leading to another insulator (Fig. 1 (a)) or split into several Weyl points resulting in a Weyl semi-metal. In the latter case, depending on whether the trajectory, traversed by the Weyl point, is closed or not, the Weyl semi-metal phase turns into another insulator (Fig. 1 (b)) or persists all the way (Fig. 1 (c)). In all three cases, at the QCP between any pair of neighboring phases, the energy dispersion near a BTP is highly anisotropic, which is linear in two directions and quadratic along the third direction. This anisotropic dispersion induces new power laws in the temperature dependence of various measurable quantities and anisotropic physical responses.

Phase transition through ABC.— In noncentrosymmetric systems, the ABC between the conduction and valence bands can be described by the following 2×2 Hamiltonian, $H(\mathbf{k}, m) = f_0(\mathbf{k}, m) + \sum_{i=1}^3 f_i(\mathbf{k}, m)\tau_i$, where $f_{0,1,2,3}$ are real functions and $\tau_{1,2,3}$ are Pauli matrices indicating the two bands. Here m describes a tuning parameter. In particular, we consider the following situation. For $m < m_c$, the system is fully gapped. An isolated BTP occurs at the critical point $(\mathbf{k}, m) = (\mathbf{k}_c, m_c)$ where $f_{1,2,3}(\mathbf{k}_c, m_c) = 0$. Since f_0 does not affect ABC, we can neglect f_0 . Then the next

question is what happens when $m > m_c$. To examine the system's behavior near the critical point, we derive the effective Hamiltonian through an expansion in powers of $\mathbf{q} = \mathbf{k} - \mathbf{k}_c$ and $\Delta m = m - m_c$. Up to the linear order of \mathbf{q} and Δm , $\mathbf{f} = (f_1, f_2, f_3)^T$ (T stands for transpose) can be written as $\mathbf{f}(\mathbf{q}, \Delta m) = \hat{M}\mathbf{q} + \Delta m\mathbf{N}$ where $\hat{M}_{ij} = \frac{\partial f_i}{\partial q_j}|_{\mathbf{q}=\Delta m=0}$ and $N_i = \frac{\partial f_i}{\partial m}|_{\mathbf{q}=\Delta m=0}$. If the determinant of \hat{M} , i.e., $\text{Det}\hat{M}$, is nonzero, the gap-closing condition $\mathbf{f} = 0$ leads to $\mathbf{q} = -\hat{M}^{-1}\mathbf{N}\Delta m$, which means that the gapless point moves as Δm varies and persists even when $\Delta m < 0$, contradicting the initial assumption. Therefore $\text{Det}\hat{M}=0$ at the PT point. In fact, the sign of $\text{Det}\hat{M} = \varepsilon_{ijk}M_{1i}M_{2j}M_{3k}$ is the chirality (or chiral charge) of the BTP at $\Delta m = 0$. Since the chirality is a topological number, a BTP with a nonzero chirality is stable against small perturbations. However, when $\text{Det}\hat{M}=0$, it is not topologically protected. Therefore when $\Delta m > 0$, the BTP can either be gapped out leading to another insulating phase or be split into several Weyl points with zero net chirality generating a stable metallic phase. When both of these possibilities are allowed, the insulating phase should be preferred since the gapped phase has lower energy.

To understand the nature of the ground state for $\Delta m > 0$, it is useful to rotate the momentum coordinate using a basis which manifests the zero chirality of the BTP at $\Delta m = 0$. Since $\text{Det}\hat{M}=0$, \hat{M} has an eigenvector \mathbf{n}_1 with zero eigenvalue satisfying $\hat{M}\mathbf{n}_1 = 0$. We introduce two additional normalized vectors $\mathbf{n}_2, \mathbf{n}_3$, which can form an orthonormal basis $\{\mathbf{n}_1, \mathbf{n}_2, \mathbf{n}_3\}$, and construct a matrix $\hat{W} = (\mathbf{n}_1, \mathbf{n}_2, \mathbf{n}_3)$. With the rotated coordinate $\mathbf{p} = \hat{W}^{-1}\mathbf{q}$, $\mathbf{f}(\mathbf{p}, \Delta m) = \mathbf{u}_2p_2 + \mathbf{u}_3p_3 + \Delta m\mathbf{N}$, where $\mathbf{u}_{2,3} = \hat{M}\mathbf{n}_{2,3}$. Here terms linear in p_1 do not appear in \mathbf{f} due to the fact that $\hat{M}\mathbf{n}_1 = 0$. Then the leading contribution of p_1 dependent term should start from quadratic order, which leads to the minimal effective Hamiltonian $H(\mathbf{p}, \Delta m) = \sum_{i=1}^3 f_i(\mathbf{p}, \Delta m)\tau_i$ in which

$$\mathbf{f}(\mathbf{p}, \Delta m) = \mathbf{u}_2p_2 + \mathbf{u}_3p_3 + \mathbf{u}_4p_1^2 + \Delta m\mathbf{N}. \quad (1)$$

Conditions to obtain an insulator.- Let us first derive the condition for IIT corresponding to Fig. 1 (a). Since the system is gapped for any $\Delta m \neq 0$, the conduction (valence) band should have a well-defined dispersion minimum (maximum) near $\mathbf{p} = 0$. Considering the minimal 2×2 Hamiltonian with $f_{1,2,3}(\mathbf{p}, \Delta m)$ in Eq. (1), the condition to have an extremum for small $\Delta m \neq 0$ leads to the following three equations $g_i = \partial E_c(\mathbf{p}, \Delta m)/\partial p_i = 0$ ($i = 1, 2, 3$). Here E_c is the energy of the conduction band. After solving the 3 coupled equations, the location of the dispersion minimum is obtained as $\mathbf{p}^{\text{min}} = (0, A\Delta m, B\Delta m)$ where A, B are some constants. This implies that across the ABC, the conduction (valence) band minimum (maximum) should move along the straight line satisfying $p_1 = 0$ and $p_2 = \frac{A}{B}p_3$ for both $\Delta m < 0$ and $\Delta m > 0$. Such a condition can be satisfied generally when the system has high crystalline symmetry along the line. Therefore the IIT is achievable when the extrema of the conduction and valence bands of the gapped phases move along a straight line across the ABC.

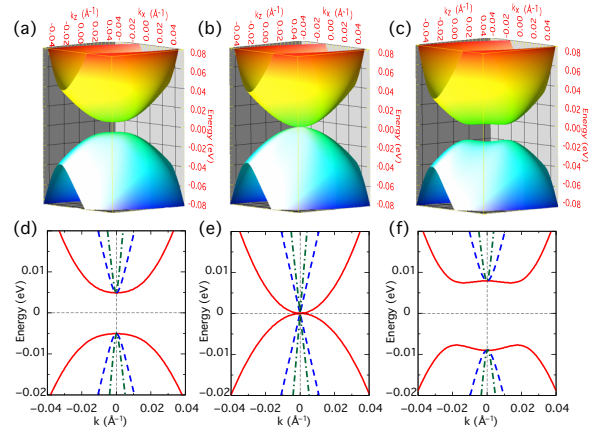


FIG. 2: (Color online) Evolution of the band structure, obtained from first-principle calculations, across the topological PT in BiTeI under pressure P . Energy dispersion of the conduction/valence bands near one of the BTP in (p_1, p_2) plane, which is normal to the high symmetry line embracing QCPs, is shown for (a) $P < P_c$, (b) $P = P_c$, (c) $P > P_c$, respectively. Energy dispersions along the p_1 (red), p_2 (green), p_3 (blue) directions are shown for (d) $P < P_c$, (e) $P = P_c$, and (f) $P > P_c$, respectively.

As a consequence of the IIT, the energy dispersion develops a peculiar structure. To understand the band shape near the dispersion minimum, we compute the Hessian matrix $\hat{H}_{ij}^{\text{min}} = \frac{\partial^2 E_c}{\partial p_i \partial p_j}$, which has a block diagonal form with $\hat{H}_{12}^{\text{min}} = \hat{H}_{13}^{\text{min}} = 0$ at $\mathbf{p} = \mathbf{p}^{\text{min}}$. The other nonzero components of \hat{H}^{min} satisfies

$$\hat{H}_{11}^{\text{min}} = c_{11}\Delta m, \quad \text{Det} \begin{pmatrix} H_{22}^{\text{min}} & H_{23}^{\text{min}} \\ H_{32}^{\text{min}} & H_{33}^{\text{min}} \end{pmatrix} > 0,$$

where c_{11} is a constant. Interestingly, $\hat{H}_{11}^{\text{min}}$ changes the sign across the PT because it is linearly proportional to Δm . For $c_{11} < 0$ ($c_{11} > 0$), the conduction band has a dispersion minimum in all three directions for $\Delta m < 0$ ($\Delta m > 0$) while it has a saddle point with a negative curvature along the p_1 direction for $\Delta m > 0$ ($\Delta m < 0$). Therefore when there is a IIT, one insulating phase should possess a saddle point at the bottom (top) of the conduction (valence) band along the p_1 direction where the energy dispersion is quadratic at QCP.

We can apply this theory to the IIT of the pressured BiTeI. [12]. In this system, ABC occurs along the high symmetry line $A-H$ in $k_z = \pi$ plane (BZ of BiTeI is shown in Fig. 1 of [12]). Because of the C_{3v} symmetry, the conduction (valence) band with Rashba-type spin-splitting develops a dispersion minimum (maximum) along this line for any pressure across the ABC, which satisfies the necessary condition for the IIT. In Fig. 2, we plot the evolution of the band dispersion across the ABC near one of BTPs using the band structure obtained by first principle calculations. [13] At the QCP, the band dispersion is quadratic along one direction and linear along the other two directions. Moreover, beyond the critical pressure, the band dispersion of the insulating phase possesses a saddle point, proving the occurrence of the IIT.

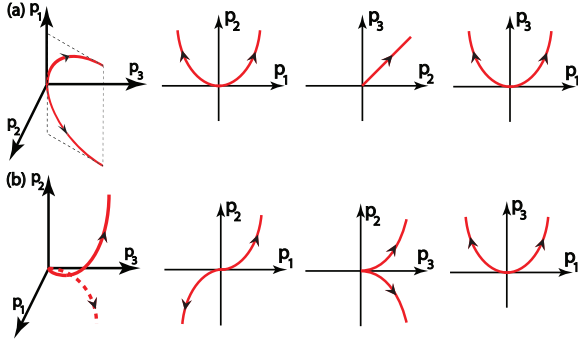


FIG. 3: (Color online) The trajectory of BTPs in 3D space and its 2D projections. (a) The curve is lying on a 2D plane leading to Fig. 1 (b). (b) The curve is moving in 3D space leading to Fig. 1 (c).

Conditions to obtain a semi-metal.— If the condition for gap reopening is not satisfied, the BTP at $\Delta m = 0$ can be split into several BTPs. Here we focus on the case of generating two BTPs with opposite chiral charges for convenience. Since there are 4 parameters ($p_{1,2,3}$ and Δm) while only 3 conditions of $f_{1,2,3} = 0$ are required to be satisfied to achieve a gapless phase, there is a line of gapless points in the $(\mathbf{p}, \Delta m)$ space in general. Regarding $t \equiv \Delta m$ as a parameter, the trajectories of the two BTPs form a curve $\mathbf{p}^*(t) = (p_1^*(t), p_2^*(t), p_3^*(t))$ in 3D momentum space. To determine the structure of the phase diagram, it is crucial to understand the shape of the curve in 3D space.

When the BTP, $\mathbf{p}^*(t = 0)$ is free of symmetry constraints, the three components of $\mathbf{p}^*(t = 0)$ are linearly independent in general. In this case, from Eq. (1), the location of BTPs for small $t > 0$ can be obtained as $\mathbf{p}^*(t) = (\pm a_1 \sqrt{t}, a_2 t, a_3 t)$ with $a_{1,2,3}$ constants, which is initially proposed by Murakami and Kuga in Ref. 8. The shape of this trajectory in 3D momentum space and its 2D projections are shown in Fig. 3 (a). Since the curve is lying on a 2D plane, the trajectory can form a closed loop, which can generate another insulating state via a pair-annihilation of BTPs. Therefore an ABC at a generic momentum point without symmetry constraints can give rise to Fig. 1 (b). [8]

On the other hand, when $\mathbf{p}^*(t = 0)$ is under symmetry constraints, the components of $\mathbf{p}^*(t = 0)$ cannot be linearly independent. For example, in BiTeI, $\mathbf{p}^*(t = 0)$ exists on a line where the Hamiltonian is invariant under the combination of time-reversal and mirror symmetries. Although the IIT should occur in this system, let us suppose that the splitting of the BTP is possible. In this case, it can be shown that the trajectory follows $\mathbf{p}^*(t) = (\pm \alpha \sqrt{t}, \pm \beta t^{3/2}, \gamma t)$ with constants α, β, γ . This is because the components $p_{1,2,3}$ of $\mathbf{p}^*(t)$ satisfy $p_2 \propto p_1 p_3$ due to the symmetry constraint at $t = 0$. The detailed derivation is provided in the Supplementary Material. The shape of this trajectory is shown in Fig. 3 (b). It is worth noting that the trajectory moves in 3D space. It is vanishingly improbable that two curves emanating from the origin and traveling in 3D space can collide again considering the

	$D(\varepsilon)$	$C_V(T)$	$\kappa(T)$	$\chi_D(T)$	$\sigma_{DC}(T)$
Weyl semi-metal	ε^2	T^3	T^2	$\ln T$	T
At the QCP	$\varepsilon^{3/2}$	$T^{5/2}$	$T^{3/2}$	$T^{-1/2}$	$T^{1/2}$

TABLE I: Temperature (or energy) dependence of various physical quantities for a 3D Weyl semi-metal and at the QCP. $D(\varepsilon)$, C_V , κ , χ_D , σ_{DC} are the density of states, specific heat, compressibility, diamagnetic susceptibility, and DC conductivity, respectively. $\sigma_{DC}(T)$ is obtained by using the T-linear scattering rate due to Coulomb interaction between electrons.

huge volume of the momentum space. Therefore if an ABC occurs at a momentum under symmetry constraints, the trajectory of BTPs can form an open curve leading to the phase diagram in Fig. 1 (c).

Topological PT.— The IIT can accompany the change of bulk topological properties. [14] In 3D systems with TRS, band insulators can be classified by Z_2 topological numbers $\nu_{0,1,2,3}$. [1, 15, 16] In the BZ, there are 3 pairs of parallel planes, in which $\mathbf{k} \cdot \mathbf{a}_i = 0$ or π . ($i = 1, 2, 3$) Here $\mathbf{a}_{1,2,3}$ are primitive lattice vectors. Since each plane has TRS, a 2D Z_2 invariant α_i^0 (α_i^π) can be assigned to the plane satisfying $\mathbf{k} \cdot \mathbf{a}_i = 0$ ($\mathbf{k} \cdot \mathbf{a}_i = \pi$). Since $\alpha_1^0 + \alpha_1^\pi = \alpha_2^0 + \alpha_2^\pi = \alpha_3^0 + \alpha_3^\pi$, only four 2D invariants are independent and determine the Z_2 invariants of the 3D system in the following way, $(\nu_0, \nu_1, \nu_2, \nu_3) = (\alpha_1^0 + \alpha_1^\pi, \alpha_1^\pi, \alpha_2^\pi, \alpha_3^\pi)$. The strong invariant ν_0 distinguishes a TI ($\nu_0 = 1$) and a band insulator ($\nu_0 = 0$). Since $\nu_0 = \alpha_i^0 + \alpha_i^\pi$ for any $i = 1, 2, 3$, if one of 2D Z_2 invariants changes by 1 through ABC, topological PT occurs.

In a 2D BZ with TRS, the Z_2 invariant α is given by the Chern number (modulo 2), which is the integral of the Berry curvature over the half BZ (with additional contraction procedures). [15] Therefore if the ABC between the valence and conduction bands, changing the Chern number of each band by ± 1 per a touching [17], occurs odd number of times in the half BZ, α changes by 1 leading to 3D topological PT. Therefore when IIT happens, if the high crystalline symmetry line embracing QCPs is on a 2D plane with TRS and the number of such lines in the half BZ is odd, a topological PT occurs. This condition is exactly satisfied in BiTeI where three high symmetry lines embracing BTPs are on the $k_z = \pi$ plane with TRS leading to the topological PT. [12]

Thermodynamic properties at QCP.— The anisotropic dispersion of the BTP with zero chirality leads to the following minimal Hamiltonian at the QCP,

$$H_{\text{QCP}}(\mathbf{p}) = A p_1^2 \tau_1 + v p_2 \tau_2 + v p_3 \tau_3. \quad (2)$$

where v is the velocity and A is the inverse mass. This gives rise to the density of states $D(\varepsilon) \propto \varepsilon^{3/2}$, which is quite distinct from that for a 3D Weyl semi-metal ($D(\varepsilon) \propto \varepsilon^2$) or a 3D normal metal with quadratic dispersion ($D(\varepsilon) \propto \varepsilon^{1/2}$). The distinct power law of $D(\varepsilon)$ directly leads to new exponents in the temperature dependence of various thermodynamic quantities such as the specific heat (C_V) and compressibility (κ) as summarized in Table I. The diamagnetic susceptibility χ_D

also shows an unexpected singular behavior. We have computed χ_D using the Fukuyama formula for the orbital susceptibility $\chi_D = \frac{e^2 T}{c^2 V} \sum_{n, \mathbf{p}} \text{Tr}[G\gamma_a G\gamma_b G\gamma_a G\gamma_b]$. [18] Here G is the Green's function, $\gamma_a \equiv \frac{\partial H_{\text{QCP}}}{\partial p_a}$ and a, b are two orthogonal directions perpendicular to the applied magnetic field. From Eq. (2), χ_D is given by $\chi_D(\theta) = \cos^2 \theta \chi_1 + \sin^2 \theta \chi_2$, in which $\chi_1 \approx C_1 T^{-1/2}$ and $\chi_2 \approx \chi_2^0 + C_2 T^{1/2}$ with χ_2^0 , $C_{1,2}$ constants. Here θ is the angle between the external magnetic field and p_1 direction. Therefore χ_D shows unusual singular temperature dependence in low temperature given by $\chi_D \sim T^{-1/2}$ irrespective of magnetic field directions.

Anisotropic DC conductivity.- The anisotropic dispersion at QCP also induces anisotropic temperature dependence of the DC conductivities. Assuming momentum independence of the scattering rate $\frac{1}{\tau(\omega)}$, a straightforward calculation of the conductivity tensor using Kubo formula gives rise to the following expression of the DC conductivities,

$$\begin{aligned} \sigma_{11}(T) &= \frac{2e^2 \sqrt{A}}{7\pi^2 v^2} \int d\omega |\omega|^{5/2} \left(-\frac{\partial f}{\partial \omega} \right) \tau(\omega), \\ \sigma_{22,33}(T) &= \frac{9e^2}{20\pi^2 \sqrt{A}} \int d\omega |\omega|^{3/2} \left(-\frac{\partial f}{\partial \omega} \right) \tau(\omega), \end{aligned} \quad (3)$$

When the Coulomb interaction between electrons dominates the scattering, we can take $\frac{1}{\tau} = \alpha^2 T$ with $\alpha = \frac{e^2}{4\pi\epsilon v}$, considering that the low temperature transport is dominated by the linear dispersion. In this case, the DC conductivity satisfies $\sigma_{11}(T) \propto T^{3/2}$ and $\sigma_{22,33}(T) \propto T^{1/2}$. On the other hand, when the scattering due to random potentials dominates the transport, using Born approximation, the leading contribution to the scattering rate can be obtained by $\frac{1}{\tau(\omega)} \approx 2\pi\gamma_0 D(\omega)$ with $\gamma_0 = \frac{n_i V_0^2}{2}$. [19] Here V_0 is the impurity scattering potential, n_i is the impurity density. Then using Eq. (3), we obtain $\sigma_{33}(T) = \frac{9e^2 v^2}{20\pi\gamma_0}$, $\sigma_{11}(T) = \frac{2e^2 A}{7\pi\gamma_0} (2 \ln 2) T$, which also shows the anisotropic T dependence. [20] In fact, Eq. (3) implies that, as long as the scattering rate is momentum independent, irrespective of the scattering mechanism $\frac{\sigma_{11}(T)}{\sigma_{33}(T)} = C_0 \frac{A}{v^2} T$ where $C_0 \approx 1.8$.

Stability of QCP.- Finally, let us discuss about the stability of the QCP against disorder and Coulomb interaction. The effective action of the QCP including both random disorder potential and $1/r$ Coulomb interaction can be written as

$$\begin{aligned} S &= \int dt d^3x [\psi^\dagger (i\partial_t + A\partial_1^2 \tau_1 + \sum_{j=2,3} iv\partial_j \tau_j) \psi + V_i \psi^\dagger M_i \psi] \\ &+ \int dt d^3x d^3x' (\psi^\dagger \psi)_{x,t} \frac{g^2}{2|\mathbf{x} - \mathbf{x}'|} (\psi^\dagger \psi)_{x',t}. \end{aligned} \quad (4)$$

where $V_i(\mathbf{x})$ is a random potential coupled to fermion field $\psi(\mathbf{x})$ via a matrix M_i . $g^2 = e^2/\epsilon$ where e and ϵ are the electric charge and dielectric constant, respectively. We take a random disorder potential with Gaussian invariance whose impurity average satisfies $\langle V_i(\mathbf{x}) V_j(\mathbf{x}') \rangle = \Delta_{ij} \delta^{(3)}(\mathbf{x} - \mathbf{x}')$. The key characteristics of the Gaussian fixed point in Eq. (2) is the invariance of the Hamiltonian under the anisotropic scaling of

spatial coordinates, i.e., $\tilde{x}_1 = x_1/b^{1/2}$, $\tilde{x}_{2,3} = x_{2,3}/b$ accompanied by $\tilde{t} = t/b$ where the tilde indicates the new scaled coordinates. Under this scale transformation, Δ_{ij} transforms as $\tilde{\Delta}_{ij} = b^{-1/2} \Delta_{ij}$ showing the irrelevance of the disorder. Similarly, we can show that $\tilde{g}^2 = g^2$, i.e., Coulomb interaction is marginal, which, however, eventually becomes irrelevant according to the one-loop perturbative renormalization group calculation. [21] Therefore the unusual power laws in various thermodynamic and transport properties, which are predicted based on the free particle Hamiltonian in Eq. (2) should persist even under the influence of the disorder and Coulomb interaction.

We greatly appreciate the stimulating discussions with Amnon Aharony, Ora Entin-Wohlman and Michael Hermele. This work is supported by the Japan Society for the Promotion of Science (JSPS) through the ‘‘Funding Program for World-Leading Innovative R&D on Science and Technology (FIRST Program)’’, and by Grant-in-Aids for Scientific Research (No. 24224009) from the Ministry of Education, Culture, Sports, Science and Technology (MEXT) of Japan.

-
- [1] L. Fu, C. L. Kane, E. J. Mele, Phys. Rev. Lett. **98**, 106803 (2007).
 - [2] X. -L. Qi, T. L. Hughes and S. -C. Zhang, Phys. Rev. B **78**, 195424 (2008).
 - [3] S. -Y. Xu et al., Science **332**, 560 (2011).
 - [4] T. Sato et al., Nat. Phys. **7**, 840 (2011).
 - [5] P. Goswami and S. Chakravarty, Phys. Rev. Lett. **107**, 196803 (2011).
 - [6] H. Isobe and N. Nagaosa, Phys. Rev. B **86**, 165127 (2012).
 - [7] P. Hosur, S. A. Parameswaran, and A. Vishwanath, Phys. Rev. Lett. **108**, 046602 (2012).
 - [8] S. Murakami and S. -i. Kuga, Phys. Rev. B **78**, 165313 (2008); S. Murakami, New J. Phys. **9**, 356 (2007).
 - [9] X. Wan, A. M. Turner, A. Vishwanath, and S. Y. Savrasov, Phys. Rev. B **83** 205101 (2011).
 - [10] K. Ishizaka et al., Nat. Mater. **10** 521 (2011).
 - [11] M. S. Bahrany, R. Arita, and N. Nagaosa, Phys. Rev. B **84** 041202(R) (2011).
 - [12] M. S. Bahrany, B. -J. Yang, R. Arita, and N. Nagaosa, Nat. Commun. **3** 679 (2012).
 - [13] Details for first-principles calculations can be found in [12].
 - [14] The condition for the topological phase transition mediated by a intervening semi-metallic phase can be found in [8].
 - [15] J. E. Moore and L. Balents, Phys. Rev. B **75**, 121306(R) (2007).
 - [16] R. Roy, Phys. Rev. B **79**, 195322 (2009).
 - [17] M. Oshikawa, Phys. Rev. B **50**, 17357 (1994).
 - [18] H. Fukuyama, Prog. Theor. Phys. **45**, 704 (1971).
 - [19] The detailed derivation procedure is provided in the Supplementary Material.
 - [20] The T linear behavior of $\sigma_{11}(T)$ due to disorder scattering implies a vanishingly small conductivity in $T \rightarrow 0$ limit. This is an artifact of the simple (non self-consistent) Born approximation. Once the self-consistency is carefully considered, $\sigma_{11}(T)$ should approach a constant value as $T \rightarrow 0$.
 - [21] B.-J. Yang et al., unpublished.
 - [22] M. Spivak, Differential Geometry vol II, Publish or Perish, Inc

(1970).

[23] P. Hosur, S. A. Parameswaran, and A. Vishwanath, Phys. Rev. Lett. **108**, 046602 (2012).

SUPPLEMENTARY MATERIAL

A curve in 3D and its curvature and torsion

In this section, we describe the relation between the shape of a curve in 3D space and its curvature and torsion. Here we basically follow the contents in Ref. 22. A convenient way to describe a curve $C = C(t) = (x(t), y(t), z(t))$ is to use an orthogonal coordinate system $(\mathbf{t}, \mathbf{n}, \mathbf{b})$ where \mathbf{t} , \mathbf{n} , \mathbf{b} are the tangential, normal, and binormal vectors, respectively. To define \mathbf{t} , \mathbf{n} , \mathbf{b} we first consider the arclength, which is defined as

$$s(t) = \int_0^t dt' \left| \frac{dC(t')}{dt'} \right|. \quad (5)$$

For the following discussion, we reparametrize the curve C using the arclength s , which makes C to be a function of s , i.e., $C = C(s)$. Then \mathbf{t} , \mathbf{n} , \mathbf{b} are given by

$$\mathbf{t} \equiv \frac{dC}{ds}, \quad \mathbf{n} \equiv \frac{d^2C}{ds^2} / \left| \frac{d^2C}{ds^2} \right|, \quad \mathbf{b} \equiv \mathbf{t} \times \mathbf{n}, \quad (6)$$

and the curvature κ_C and torsion τ_C are defined as

$$\kappa_C(s) \equiv \left| \frac{d\mathbf{t}}{ds} \right|, \quad \frac{d\mathbf{b}}{ds} \equiv -\tau_C(s)\mathbf{n}. \quad (7)$$

Therefore κ_C measures the rate at which the tangential vector changes and τ_C measures the rate at which the curve C deviates from being a planar curve lying on the (\mathbf{t}, \mathbf{n}) space. In the case of the torsion τ_C , it has a following equivalent expression,

$$\tau_C = \frac{1}{\kappa_C^2} \left\langle \frac{dC}{ds} \times \frac{d^2C}{ds^2}, \frac{d^3C}{ds^3} \right\rangle, \quad (8)$$

where $\langle A, B \rangle$ indicates the inner product of two vectors A and B .

The relation between the shape of a curve and its curvature and torsion can be understood by considering two dimensional projections of the curve on the planes in which two vectors among $\{\mathbf{t}, \mathbf{n}, \mathbf{b}\}$ are adopted as a basis. To represent an arbitrary curve $C(s)$ we can choose a coordinate which satisfies $C(0) = 0$, $\left. \frac{dC}{ds} \right|_{s=0} = (1, 0, 0)$, and $\left. \frac{d^2C}{ds^2} \right|_{s=0} = (0, \kappa_C, 0)$. Then from Eq. (8), we obtain $\left. \frac{d^3C}{ds^3} \right|_{s=0} = (a_1, a_2, \kappa_C \tau_C)$ where $a_{1,2}$ are arbitrary numbers.

Now we consider the Taylor expansion of $C(s) = (x(s), y(s), z(s))$ at $s = 0$,

$$C(s) = C(0) + s \left. \frac{dC}{ds} \right|_0 + \frac{s^2}{2} \left. \frac{d^2C}{ds^2} \right|_0 + \frac{s^3}{6} \left. \frac{d^3C}{ds^3} \right|_0 + O(s^4), \quad (9)$$

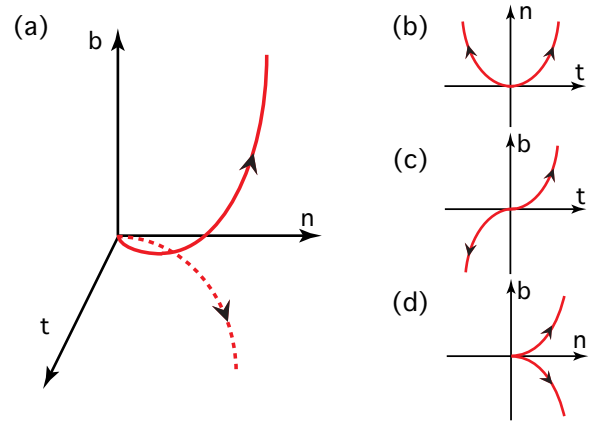


FIG. 4: (Color online) (a) Typical shape of a curve with nonzero curvature and torsion in 3D space. 2D Projections of the curve onto (b) (\mathbf{t}, \mathbf{n}) plane, (c) (\mathbf{t}, \mathbf{b}) plane, (d) (\mathbf{n}, \mathbf{b}) plane. Here two arrows describe the flowing directions of two band touching points which are generated from the QCP at the origin.

which gives rise to

$$\begin{aligned} x(s) &= s + O(s^3), \\ y(s) &= \frac{\kappa_C}{2} s^2 + O(s^3), \\ z(s) &= \frac{\kappa_C \tau_C}{6} s^3 + O(s^4). \end{aligned} \quad (10)$$

From the leading order terms, the projections of the curve C are described by $y = \frac{\kappa_C}{2} x^2$, $z = \frac{\kappa_C \tau_C}{6} x^3$, and $z^2 = \frac{2}{9} \frac{\tau_C^2}{\kappa_C} y^3$, which are lying on (\mathbf{t}, \mathbf{n}) , (\mathbf{t}, \mathbf{b}) , and (\mathbf{n}, \mathbf{b}) planes, respectively. A typical example of a curve in 3D and its 2D projections are shown in Fig. 4. It is to be noted that the projections of the curve on (\mathbf{t}, \mathbf{b}) and (\mathbf{n}, \mathbf{b}) planes, shown in Fig. 4 (c) and (d), respectively, cannot form a closed curve under smooth variations of the curve. Since the shapes of these 2D projections remain the same as long as the torsion is nonzero at the origin, we obtain the zero torsion condition $\tau_C = 0$ to form a closed curve. On the other hand, when $\tau_C = 0$, the curve moves on the 2D space spanned by (\mathbf{t}, \mathbf{n}) . The trajectory of the curve on (\mathbf{t}, \mathbf{n}) plane shown in Fig. 4 (b) can make a closed loop as long as the curvature κ_C is finite.

Effective Hamiltonian for topological phase transition in BiTeI

Let us first consider a general Hamiltonian defined in momentum space $H(\mathbf{k}) = H(k_x, k_y, k_z)$. Then the combined symmetry operation TM , which is the combination of the time reversal (T) and mirror ($M : y \rightarrow -y$), imposes the following constraint to the $H(\mathbf{k})$,

$$\begin{aligned} (TM)H(k_x, k_y, k_z)(TM)^{-1} \\ = H^*(k_x, k_y, k_z) = H(-k_x, k_y, -k_z). \end{aligned} \quad (11)$$

Assuming that the band touching point exists at $\mathbf{k}_c = (0, k_{y,c}, \pi)$, we derive the low energy Hamiltonian considering small momentum deviation from the band touching point.

Due to the TM symmetry, the effective 2×2 Hamiltonian $H_{2 \times 2}(\mathbf{q})$ with $\mathbf{q} = \mathbf{k} - \mathbf{k}_c$, satisfies the following constraint,

$$\begin{aligned}
(TM)H_{2 \times 2}(q_x, q_y, q_z)(TM)^{-1} &= H_{2 \times 2}^*(q_x, q_y, q_z) \\
&= H_{2 \times 2}^*(k_x, k_y - k_{y,c}, k_z - \pi) \\
&= H_{2 \times 2}(-k_x, k_y - k_{y,c}, -k_z - \pi) \\
&= H_{2 \times 2}(-k_x, k_y - k_{y,c}, -k_z + \pi) \\
&= H_{2 \times 2}(-q_x, -q_y, -q_z).
\end{aligned} \tag{12}$$

Therefore

$$H_{2 \times 2}^*(q_x, q_y, q_z) = H_{2 \times 2}(-q_x, -q_y, -q_z) \tag{13}$$

For the generic 2×2 Hamiltonian $H_{2 \times 2}(\mathbf{q})$ given by,

$$H_{2 \times 2}(\mathbf{q}) = f_1(\mathbf{q})\tau_1 + f_2(\mathbf{q})\tau_2 + f_3(\mathbf{q})\tau_3, \tag{14}$$

the constraint in Eq. (13) leads to the following constraints to $f_{1,2,3}(\mathbf{q})$,

$$\begin{aligned}
f_{1,3}(-q_x, q_y, -q_z) &= f_{x,z}(q_x, q_y, q_z) \\
f_2(-q_x, q_y, -q_z) &= -f_y(q_x, q_y, q_z)
\end{aligned} \tag{15}$$

which means that $f_{1,3}$ (f_2) are even (odd) under the simultaneous sign change of q_x and q_z . Now we expand $f_{1,2,3}$ near the band touching point at $\mathbf{q} = 0$ and $P = P_c$ in the powers of $q_{x,y,z}$ and $\Delta P = P - P_c$. Due to the symmetry constraint in Eq. (15), up to linear order in $q_{x,y,z}$ and $\Delta P = P - P_c$, $f_{1,2,3}$ are given by

$$\begin{aligned}
f_1 &= N_1 \Delta P + M_{12} q_y \\
f_2 &= M_{21} q_x + M_{23} q_z \\
f_3 &= N_3 \Delta P + M_{32} q_y
\end{aligned} \tag{16}$$

where $N_{1,3}$ and $M_{12,21,23,32}$ are constants. The Hamiltonian at the critical point $\Delta P = 0$ can be written as

$$H_{2 \times 2}(\mathbf{q}) = M_{12} q_y \tau_1 + (M_{21} q_x + M_{23} q_z) \tau_2 + M_{32} q_y \tau_3, \tag{17}$$

Since $\text{Det}M = 0$, M always has an eigenvector ξ_1 with zero eigenvalue. Explicitly, $\xi_1^t = \frac{1}{\sqrt{M_{21}^2 + M_{23}^2}}(-M_{23}, 0, M_{21})$ where the superscript t means the transpose of a vector.

Let us introduce $\xi_2^t = \frac{1}{\sqrt{M_{21}^2 + M_{23}^2}}(M_{21}, 0, M_{23})$ and $\xi_3^t = (0, 1, 0)$. Then $\xi_{1,2,3}$ constitute an orthogonal basis. Using this, we consider following linear transformation,

$$\begin{aligned}
\begin{pmatrix} q_x \\ q_y \\ q_z \end{pmatrix} &\equiv (\xi_1, \xi_2, \xi_3) \begin{pmatrix} p_1 \\ p_2 \\ p_3 \end{pmatrix} \\
&= \begin{pmatrix} \frac{-M_{23}}{\sqrt{M_{21}^2 + M_{23}^2}} p_1 + \frac{M_{21}}{\sqrt{M_{21}^2 + M_{23}^2}} p_2 \\ p_3 \\ \frac{M_{21}}{\sqrt{M_{21}^2 + M_{23}^2}} p_1 + \frac{M_{23}}{\sqrt{M_{21}^2 + M_{23}^2}} p_2 \end{pmatrix}
\end{aligned} \tag{18}$$

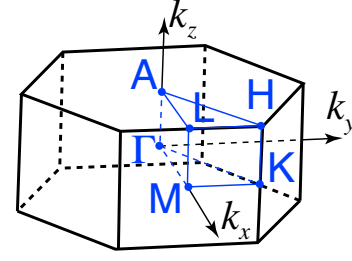


FIG. 5: (Color online) The hexagonal Brillouin zone of BiTeI.

Applying the above linear transformation, the Hamiltonian is given by $H_{2 \times 2}(\mathbf{p}) = \sum_{i=1,2,3} f_i(\mathbf{p})\tau_i$ in which

$$\begin{aligned}
f_1 &= N_1 \Delta P + M_{12} p_3, \\
f_2 &= \sqrt{M_{21}^2 + M_{23}^2} p_2, \\
f_3 &= N_3 \Delta P + M_{32} p_3.
\end{aligned} \tag{19}$$

It is to be noticed that p_1 does not appear in the Hamiltonian due to the fact the ξ_1 is the eigenvector of M with zero eigenvalue.

To fully account for the phase transition, the terms quadratic in p_i are necessary. In terms of the rotated momentum \mathbf{p} , the symmetry constraint in Eq. (15) can be written as

$$H_{2 \times 2}(p_1, p_2, p_3) = H_{2 \times 2}(-p_1, -p_2, p_3). \tag{20}$$

Collecting terms satisfying the constraint above up to the quadratic order in p_i , $f_{1,2,3}$ can be written as

$$\begin{aligned}
f_1 &= N_1 \Delta P + M_{12} p_3 + a_1 p_1^2 + a_2 p_2^2 + a_3 p_3^2 + a_4 p_1 p_2, \\
f_2 &= \sqrt{M_{21}^2 + M_{23}^2} p_2 + b_5 p_2 p_3 + b_6 p_3 p_1, \\
f_3 &= N_3 \Delta P + M_{32} p_3 + c_1 p_1^2 + c_2 p_2^2 + c_3 p_3^2 + c_4 p_1 p_2,
\end{aligned} \tag{21}$$

where a_i, b_i, c_i ($i = 1, 2, \dots, 6$) are constants.

Topological phase transition in BiTeI

Recently, it is shown that when external pressure is applied to BiTeI, a direct phase transition from a normal insulator to a TI occurs mediated by accidental band touching points at the critical pressure $P = P_c$. The nature of the topological phase transition in BiTeI can be understood based on the general considerations developed in previous discussions. The key ingredient to understand the phase transition in this material is the fact that in the BZ shown in Fig. 5, the band touching occurs along the $A - H$ direction in $k_z = \pi$ plane, along which the Hamiltonian $H(\mathbf{k})$ is invariant under the combination of the time reversal (T) and mirror (M) symmetries. Picking one of the $A - H$ direction along the k_y axis, the combined symmetry operation TM imposes the following constraint

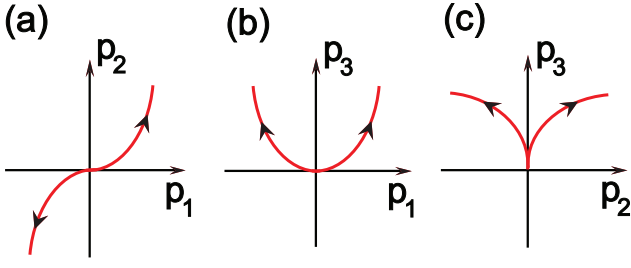


FIG. 6: (Color online) The 2D projections of the curve satisfying the gap-closing condition for the trajectory in Eq. (23) for $\alpha > 0$, $\beta > 0$, $\gamma > 0$.

to the Hamiltonian, $H^*(k_x, k_y, k_z) = H(-k_x, k_y, -k_z)$ because the mirror M changes k_y to $-k_y$. This symmetry constraint restricts the structure of the low energy Hamiltonian near the gap-closing points. Explicitly, the effective Hamiltonian near one of the band touching points can be written as $H(\mathbf{p}, \Delta P) = \sum_{i=1}^3 f_i(\mathbf{p}, \Delta P)\tau_i$ in which

$$\begin{aligned} f_1 &= N_1\Delta P + M_{12}p_3 + a_1p_1^2 + a_2p_2^2 + a_3p_3^2 + a_4p_1p_2, \\ f_2 &= \sqrt{M_{21}^2 + M_{23}^2}p_2 + b_5p_2p_3 + b_6p_3p_1, \\ f_3 &= N_3\Delta P + M_{32}p_3 + c_1p_1^2 + c_2p_2^2 + c_3p_3^2 + c_4p_1p_2, \end{aligned} \quad (22)$$

where a_i, b_i, c_i ($i = 1, 2, \dots, 6$) are constants and $\Delta P = P - P_c$. \mathbf{p} is the rotated momentum coordinates adapted to manifest the zero chirality of the band touching point. Therefore the terms linear in p_1 do not appear in $f_{1,2,3}$. The detailed procedures to derive the above Hamiltonian is shown in the Supplementary Material.

Let us first check the conditions to obtain a semi-metallic phase by finding the solution of $f_{1,2,3} = 0$. When $|\mathbf{p}| \ll 1$, $f_2 = 0$ leads to, $p_2 \propto p_3p_1$. Inserting this result to the conditions $f_{1,2} = 0$, the general solution of the gapless point has the following structure, $p_1^* = \pm\alpha\sqrt{\Delta P}$, $p_2^* = \pm\beta(\Delta P)^{3/2}$, $p_3^* = \gamma\Delta P$ with α, β, γ constants. Here we assume that the gapless point exists only for $\Delta P > 0$. Therefore the trajectory of the gapless points is given by

$$p^* = (\pm\alpha\sqrt{\Delta P}, \pm\beta(\Delta P)^{3/2}, \gamma\Delta P) \quad (23)$$

whose curvature and torsion at $\Delta P = 0$ is given by $\kappa_C = \frac{2\gamma}{\alpha^2}$ and $\tau_C = \frac{-3\beta}{\alpha\gamma}$, respectively. Since the curve has a finite torsion, we expect the trajectory of the gapless points would not form a closed loop under the smooth variation of the system, which is supported by the corresponding 2D projections of the curve shown in Fig. 6. Therefore once a semi-metallic phase occurs by splitting the band touching point at $\Delta P = 0$, the gapless point should persist for all ΔP , which is not consistent with the predictions of the first principle calculation.

The only way to describe the transition between two insulators is the occurrence of the direct transition between them via band touching at a single critical point. From the condition that the conduction band has a minimum, we have three

equations of $\frac{\partial E_c(\mathbf{p})}{\partial p_i} = 0$ ($i = 1, 2, 3$). After careful examination of the three coupled equations, we have found that there is a unique solution given by

$$\mathbf{p}^{\min} = (0, 0, -\frac{N_1M_{12} + N_3M_{32}}{M_{12}^2 + M_{32}^2}\Delta P). \quad (24)$$

Therefore the direct transition between two gapped phases requires that the extrema of the valence and conduction bands move along a particular direction, the p_3 direction throughout the phase transition. Interestingly, the p_3 direction corresponds to the k_y direction of the original coordinate, which is nothing but one of the $A - H$ direction in the BZ. Because of the C_{3v} point group symmetry, the conduction (valence) band with the Rashba-type spin-orbit coupling develops a dispersion minimum (maximum) along the $A - H$ line for any $\Delta P \neq 0$. Moreover, since the $A - H$ line is on the $k_z = \pi$ plane satisfying the time-reversal invariance, the band touching can induce the topological phase transition. Explicitly, in the $k_z = \pi$ plane, the effective Hamiltonian near a gap-closing point can be written as a two dimensional massive Dirac Hamiltonian, in which ΔP plays the role of the mass term. Therefore a band touching point can change the Z_2 invariant on the $k_z = \pi$ plane by 1 through the sign change of ΔP . Since there are 3 pairs of band touching points on the same plane, the strong index ν_0 changes by 1 reflecting the emergence of the TI through the band touching.

The Hessian matrix $\hat{H}_{ij}^{\min} = \frac{\partial^2 E_c}{\partial p_i \partial p_j}$ has a block diagonal form with $\hat{H}_{13}^{\min} = \hat{H}_{23}^{\min} = 0$ at $\mathbf{p} = \mathbf{p}^{\min}$. The other nonzero components of \hat{H}^{\min} satisfies

$$\hat{H}_{33}^{\min} > 0, \quad \text{Det} \begin{pmatrix} H_{11}^{\min} & H_{12}^{\min} \\ H_{21}^{\min} & H_{22}^{\min} \end{pmatrix} = C'\Delta P,$$

where C' is a constant. Therefore the conduction band always has a minimum along the p_3 direction. On the other hand, the determinant of the Hessian matrix for the p_1, p_2 directions, normal to the $A - H$ line, shows sign change across the phase transition, which predicts the appearance of a saddle point in (p_1, p_2) plane for one of the gapped phase. Since the normal insulator for $\Delta P < 0$ possesses the conventional dispersion minimum or maximum, we can set $C' < 0$. Therefore the TI should possess saddle points in energy dispersion. The change of the band dispersion across the topological phase transition is explicitly shown in Fig. 3 of the main text from the band structure obtained by first principle calculation.

DC conductivity at the quantum critical point

Regarding the conductivity at the quantum critical point, there are two important characteristics of BiTeI as compared to the isotropic 3D Dirac semi-metal system. One is the enhanced density of states ($D(\epsilon) \propto \epsilon^{3/2}$), which can be contrasted with the 3D Dirac system ($D(\epsilon) \propto \epsilon^2$), and the other is the strong spatial anisotropy.

Influence of enhanced density of states.- Let us first consider the influence of the enhanced density of states using the semi-classical Boltzmann theory. In the case of isotropic systems with constant scattering rates, the longitudinal DC conductivity is given by

$$\sigma = \frac{e^2 v_F^2}{3} \int_{-\infty}^{\infty} d\epsilon D(\epsilon) \left[-\frac{\partial n_F(\epsilon)}{\partial \epsilon} \right] \tau. \quad (25)$$

After plugging the density of states at the quantum critical point given by

$$D(\epsilon) = \frac{1}{2\pi^2 v^2 \sqrt{A}} \epsilon^{3/2}, \quad (26)$$

the conductivity can be obtained as

$$\sigma = \frac{e^2 v_F^2}{3} \frac{1}{2\pi^2 v^2 \sqrt{A}} \left[\frac{3}{4} (2 - \sqrt{2}) \sqrt{\pi} \zeta\left(\frac{3}{2}\right) \right] (k_B T)^{3/2} \tau, \quad (27)$$

When the electron scattering is dominated by Coulomb interaction between electrons, the scattering rate $\frac{1}{\tau}$ can be estimated in the following way,

$$\frac{1}{\tau} \equiv -2\text{Im}\Sigma^{\text{ret}}(k, \omega) \approx \alpha^2 T. \quad (28)$$

The structure of τ from the Coulomb scattering can be understood in the following way. At first, according to the Fermi-Golden rule, the scattering rate should be proportional to the square of the scattering amplitude α . In addition, since there is no energy scale other than the temperature at the critical point, which immediately gives rise to the above form of τ . Then the temperature dependence of the DC conductivity is given by

$$\sigma \propto T^{3/2} \tau = \frac{T^{1/2}}{\alpha^2}, \quad \rho \propto \frac{1}{T^{1/2}}, \quad (29)$$

where ρ is the longitudinal resistivity. This can be contrasted with the corresponding quantities of the 3D Dirac semi-metal phase. [23]

$$\sigma \propto T^2 \tau = \frac{T}{\alpha^2}, \quad \rho \propto \frac{1}{T}. \quad (30)$$

Anisotropic DC conductivity.- Now let us calculate the conductivity rigorously using Kubo formula considering the anisotropic dispersion at the quantum critical point. The effective Hamiltonian at the quantum critical point is given by

$$H(\mathbf{k}) = Ak_1^2 \tau_1 + v(k_2 \tau_2 + k_3 \tau_3), \quad (31)$$

where $\tau_{1,2,3}$ are Pauli matrices representing the valence and conduction bands that touch at the critical point. v is the velocity and A is the inverse mass along the k_1 direction.

Kubo formula for frequency dependent conductivity is given by

$$\sigma_{\mu\nu}(\omega, T) = -\frac{\text{Im}\Pi_{\mu\nu}^{\text{ret}}(\omega, T)}{\omega}, \quad (32)$$

where

$$\Pi_{\mu\nu}(i\nu_n) = \frac{1}{\beta} \sum_{i\omega_n} \int \frac{d^3 k}{(2\pi)^3} \text{Tr} \left[G_{\mathbf{k}, \omega_n + \nu_n} j_\mu(\mathbf{k}) G_{\mathbf{k}, \omega_n} j_\nu(\mathbf{k}) \right]. \quad (33)$$

Here G is the Matsubara Green's function and j_μ is the current operator along the μ direction. After some calculation, we can obtain the following expressions for current-current correlations,

$$\begin{aligned} \text{Im}\Pi_{11}^{\text{ret}}(\nu, T) &= 2e^2 A^2 \int \frac{d^3 k}{(2\pi)^3} k_1^2 \int \frac{d\varepsilon}{\pi} [n_F(\varepsilon + \nu) - n_F(\varepsilon)] \\ &\times \sum_{\lambda, \lambda'} \text{Im}\mathcal{G}_\lambda^{\text{ret}}(k, \varepsilon + \nu) \text{Im}\mathcal{G}_{\lambda'}^{\text{ret}}(k, \varepsilon) \left\{ 1 - \lambda\lambda' \frac{(v^2 k_\perp^2 - A^2 k_1^4)}{E^2} \right\}, \end{aligned} \quad (34)$$

and

$$\begin{aligned} \text{Im}\Pi_{22,33}^{\text{ret}}(\nu, T) &= \frac{e^2 v^2}{2} \int \frac{d^3 k}{(2\pi)^3} \int \frac{d\varepsilon}{\pi} [n_F(\varepsilon + \nu) - n_F(\varepsilon)] \\ &\times \sum_{\lambda, \lambda'} \text{Im}\mathcal{G}_\lambda^{\text{ret}}(k, \varepsilon + \nu) \text{Im}\mathcal{G}_{\lambda'}^{\text{ret}}(k, \varepsilon) \left\{ 1 - \lambda\lambda' \frac{A^2 k_1^4}{E^2} \right\}, \end{aligned} \quad (35)$$

where $\lambda = \pm$ indicates the positive/negative energy states and $E(\mathbf{k}) = \sqrt{v^2 k_\perp^2 + A^2 k_1^4}$ with $k_\perp^2 = k_2^2 + k_3^2$. Also the imaginary part of the retarded Green's function is given by

$$\text{Im}\mathcal{G}_\lambda^{\text{ret}}(k, \varepsilon) = \frac{-\Gamma}{(\varepsilon - \lambda E(\mathbf{k}))^2 + \Gamma^2}. \quad (36)$$

After some complicate computations, we obtain the following expression of the DC conductivity due to Coulomb interaction between electrons.

$$\begin{aligned} \sigma_{11}(T) &= \frac{e^2 \sqrt{A}}{7\pi^2 v^2 \Gamma} c_{11} (k_B T)^{5/2} \propto T^{3/2}, \\ \sigma_{22,33}(T) &= \frac{9e^2}{40\pi^2 \sqrt{A} \Gamma} c_{22,33} (k_B T)^{3/2} \propto T^{1/2}, \end{aligned} \quad (37)$$

where $c_{11,22,33}$ are constants. It is to be noted that the in-plane conductivity ($\sigma_{22,33}$) follows the power law expected for the density of states at the quantum critical point. However, $\sigma_{11}(T)$ shows a completely different power law.

DC conductivity due to disorder.- Let us study the conductivity at the quantum critical point due to charge-neutral point scatterers. For this purpose, we compute the imaginary part of the electron self-energy due to disorder using Born approximation. The result is like the following.

$$\begin{aligned} \frac{1}{\tau_\lambda(\mathbf{k}, w)} &\equiv -2\text{Im}\Sigma_\lambda^{\text{ret}}(\mathbf{k}, w) \\ &= \pi n_i V_0^2 \left(D(w) + \frac{Ak_1^2}{v^2 k_\perp^2 + A^2 k_1^4} \frac{\lambda}{6\pi^2 v^2 A^{1/2} |w|^{3/2} \text{sgn}(w)} \right) \\ &= \pi n_i V_0^2 \frac{|w|^{3/2}}{2\pi^2 v^2 A^{1/2}} \left(1 + \frac{\lambda}{3} \text{sgn}(w) \frac{Ak_1^2}{v^2 k_\perp^2 + A^2 k_1^4} \right) \end{aligned} \quad (38)$$

where V_0 is the impurity scattering potential. $D(w)$ is the density of states. In contrast to the isotropic systems, the scattering rate shows a momentum dependence. However, we have to take into account of the fact that the linear dispersion dominates the low energy properties of the system over the quadratic part, which is also supported by the one-loop renormalization group calculation. [21] Therefore we can safely neglect the momentum dependence of the electron self-energy. Then the scattering rate is just proportional to the density of states, which can be written as

$$\frac{1}{\tau_\lambda(\mathbf{k}, w)} = \frac{1}{\tau(w)} = 2\pi\gamma_0 D(w), \quad \gamma_0 = \frac{n_i V_0^2}{2}, \quad (39)$$

which leads to

$$\sigma_{11}(T) = \frac{2e^2 A}{7\pi\gamma_0} (2 \ln 2) T, \quad \sigma_{22,33}(T) = \frac{9e^2 v^2}{20\pi\gamma_0}. \quad (40)$$

Here $\sigma_{22,33}(T)$ is temperature independent, which is usually

the case of isotropic systems. However, $\sigma_{11}(T)$ shows T linear behavior.

In fact, as long as the scattering rate does not show any momentum dependence, $\sigma_{11}(T)/\sigma_{33}(T)$ shows a universal behavior given by

$$\frac{\sigma_{11}(T)}{\sigma_{33}(T)} = C_0 \frac{A}{v^2} T, \quad C_0 = \frac{40 \int dx (-\frac{df}{dx}) |x|^{5/2}}{63 \int dx (-\frac{df}{dx}) |x|^{3/2}} \approx 1.8, \quad (41)$$

where

$$\begin{aligned} \sigma_{11}(T) &= \frac{2e^2 \sqrt{A}}{7\pi^2 v^2} \int d\varepsilon |\varepsilon|^{5/2} \left(-\frac{\partial f}{\partial \varepsilon} \right) \tau(\varepsilon) \\ \sigma_{33}(T) &= \frac{9e^2}{20\pi^2 \sqrt{A}} \int d\varepsilon |\varepsilon|^{3/2} \left(-\frac{\partial f}{\partial \varepsilon} \right) \tau(\varepsilon). \end{aligned} \quad (42)$$